Article

Gasification of Lower Monohydric Alcohols by Solution Plasma Treatment and Its Reaction Mechanism

Takaki Miyamoto [ID]**, Eiji Minami *** [ID] **and Haruo Kawamoto** [ID]

Graduate School of Energy Science, Kyoto University, Yoshida-Honmachi, Sakyo-Ku, Kyoto 606-8501, Japan; miyamoto.takaki.62r@st.kyoto-u.ac.jp (T.M.); kawamoto@energy.kyoto-u.ac.jp (H.K.)
* Correspondence: minami@energy.kyoto-u.ac.jp; Tel.: +81-75-753-5713

Abstract: Solution plasma is a gas-phase discharge in the vapor bubbles in a solution and has the potential to efficiently produce H_2 by decomposing aqueous alcohols. However, the mechanism of alcohol decomposition in solution plasma remains unclear. In this study, lower monohydric alcohols (methanol and ethanol, as well as 1- and 2-propanol) were treated in solution plasma, and in this paper, the gasification mechanism is discussed. The gases produced from these alcohols were mainly H_2 and CO, with small ratios of C_1–C_3 hydrocarbons. Thus, the O/C ratio in the product gas was close to 1 for all alcohols, and most of the C atoms in the alcohols were bonded to O atoms. This excess of O atoms could have only come from water, suggesting a strong contribution of OH radicals from water for gasification. However, the C_1–C_3 hydrocarbons were produced solely by the decomposition of the alcohol. For both decomposition routes, possible reaction pathways are proposed that are consistent with the experimental facts such as the composition of the product gas and the intermediates detected.

Keywords: solution plasma; hydrogen production; gasification; methanol; ethanol; propanol

1. Introduction

The world's consumption of fossil resources continues to increase, and the resulting increase in atmospheric carbon dioxide concentration has become a substantial problem. To attain a carbon-neutral society, hydrogen energy (which has low environmental impact) is an active area of research. Currently, hydrogen is mainly produced by the steam reforming of natural gas or petroleum. However, renewable hydrogen production by the steam reforming of bioethanol [1], electrolysis of water with renewable electricity [2], or pyrolysis gasification of biomass [3] is more desirable from a sustainability standpoint.

In this context, plasma technology is a candidate for efficient hydrogen production. Plasma is a fully or partially ionized, yet electrically quasi-neutral, gas. Plasma contains radical species, positive ions, and high-energy electrons, which give it high chemical reactivity. Plasma can facilitate the decomposition and gasification of various organic materials including biomass. Biomass gasification by using atmospheric pressure plasma technologies, such as microwave plasma and dielectric barrier discharge plasma, has been extensively studied in recent years [4–6].

However, bioethanol can be used not only as a liquid fuel for automobiles, but also as a hydrogen carrier. Hydrogen production by the catalytic steam reforming of ethanol with Rh or Ni has been widely studied [7]. Hydrogen production by noncatalytic reforming of bioethanol with atmospheric pressure plasma has also been widely reported [8–10]. Plasma generated in water, termed solution plasma or in-liquid plasma, has the potential to produce hydrogen from ethanol more efficiently compared with the aforementioned methods. Solution plasma is broadly defined as plasma in contact with a liquid. Solution plasma, which is similar to conventional plasma, can facilitate various reactions using its high-energy electrons and radical species. In particular, solution plasma is characterized by its ability

to promote oxidative decomposition by OH radicals derived from water [11]. Therefore, solution plasma is expected to have various applications such as the decomposition of toxic compounds in water [12], synthesis of nanoparticles [13], and surface modification [14]. Solution plasma treatment can be performed with a variety of solvents, but water is one of the easiest solvents to use. This is because organic solvents can decompose during solution plasma treatment, sometimes producing solid carbonized substances.

In 1997, Sun et al. generated various radicals by pulsed streamer corona discharge in water [15] and investigated the effects of solution plasma on various organic compounds. They reported several cases of hydrogen production by pulsed and microwave discharges in aqueous ethanol [16–20] and further discussed the reaction pathways by analyzing the correlation between the reactive species in solution plasma and the produced gases [21]. Li et al. modulated the discharge mode by changing the angle between the electrodes placed in aqueous ethanol and evaluated the corresponding decomposition behavior of ethanol [22]. Franclemont et al. obtained H_2 and CO by generating pulsed discharges in neat methanol [23], and Shiraishi et al. improved the hydrogen production rate through the solution plasma treatment of aqueous methanol by using catalytic electrode materials [24]. The influence of the electrode material was also mentioned by Xin et al. [25]. Xin et al. also reported that in alternating current (AC) discharges, the formation of vapor bubbles by Joule heating prior to discharge initiation facilitated the production of hydrogen from aqueous methanol [26].

As aforementioned, there have been interesting studies on hydrogen production from methanol and ethanol by using solution plasma, but there have not been as many studies on solution plasma when compared with the number of studies on atmospheric pressure plasma. In addition, the gasification mechanism remains unclear. Therefore, in this study, aqueous lower monohydric alcohols (methanol, ethanol, 1-propanol, and 2-propanol) were treated in solution plasma at various concentrations. Furthermore, in this paper, the decomposition mechanisms in solution plasma are discussed based on the changes in the gasification rate and product gas composition.

2. Materials and Methods

2.1. Materials

Methanol (MeOH, >99.8%, guaranteed reagent [GR]), ethanol (EtOH, >99.5%, GR), 1-propanol (1-PrOH, >99.5%, GR), and 2-propanol (2-PrOH. >99.7%, GR) were purchased from Nacalai Tesque, Inc., Kyoto, Japan and used as received without purification. Deionized water was prepared by using an ultrapure water production system (Milli-Q Integral 3, Merck Millipore, Burlington, MA, USA) and degassed for 10 min by using aspiration and ultrasonic irradiation to remove dissolved CO_2. Sodium chloride (>99.5%, extra pure reagent [EP], Nacalai Tesque) was dissolved in this degassed deionized water as an electrolyte at a concentration of 0.1 g/L. This water was mixed with these alcohols to prepare aqueous alcohol solutions in various proportions. In this paper, alcohol concentration is expressed as the weight percent of alcohol per resulting aqueous alcohol solution.

2.2. Solution Plasma Treatment

A sealed solution plasma reactor (Figure 1a) consisting of a 100 mL Pyrex glass bottle and a pair of tungsten-rod electrodes (outer diameter: 1.0 mm) insulated with ceramic tubes was used. The ceramic tubes were used to provide a high impedance between the electrodes by insulating unnecessary conductive paths, thus facilitating electrical discharges. The details of the reaction system were described in our previous report [27]. In this reactor, 100 mL of the aqueous alcohol solution was added, and AC high-voltage pulses (MPP04-A4-30, Kurita Manufacturing Co., Ltd., Kyoto, Japan; switching frequency: 30 kHz; pulse width: 0.8 µs; no-load voltage: ± 4 kV$_{0-p}$) were applied to the electrodes to generate solution plasma for 10 min. When the high-voltage pulses were applied, vapor bubbles were generated by Joule heating between the electrodes, and gas-phase discharges occurred in the bubbles. Although the discharge power increased as the distance between the tips of

the electrodes increased [27], in this study the distance was set at approximately 1.0 mm and the average discharge power was approximately 20 W. The tip of the thermocouple was fixed approximately 1 cm below the surface of the solution to measure the solution temperature. To avoid the excessive temperature rise of the solution, the solution was circulated at 5 mL/min during the experiment and cooled by a coiled heat-exchanger placed in a water bath. To prevent the formation of nitric acid from atmospheric N_2, the empty space in the reactor was filled with Ar gas (>99.9995%, Imamura Sanso Corp., Otsu, Japan) before the experiment. A 3-L gas bag was used to collect the product gas.
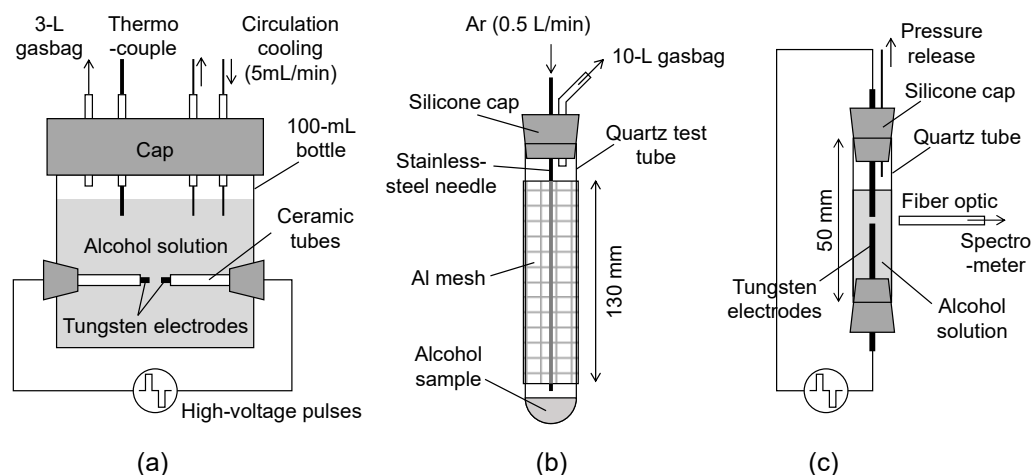

Figure 1. Schematics of (**a**) solution plasma reactor, (**b**) atmospheric pressure plasma reactor, and (**c**) apparatus for solution plasma emission spectroscopy.

2.3. Atmospheric Pressure Plasma Treatment

For comparison with the solution plasma treatment of alcohols, each neat alcohol was treated in atmospheric pressure plasma generated by dielectric barrier discharge. The experimental apparatus consisted of a quartz test tube (inner diameter: 18 mm; outer diameter: 20 mm; height: 165 mm), a stainless-steel needle (inner diameter: 1.1 mm; outer diameter: 1.5 mm; length: 200 mm) that served as a high-voltage electrode, and an aluminum mesh that served as a ground electrode wrapped 130 mm-wide around the test tube (Figure 1b). Approximately 100 mg of the alcohol sample was placed in the bottom of the test tube. Carrier gas (Ar, 0.5 L/min) was introduced through the stainless-steel needle, and AC high-voltage pulses (MPP04-A7A-30, Kurita Manufacturing Co., Ltd.; pulse width: 0.56 μs; frequency: 20 kHz; no-load voltage: 7 $kV_{0–p}$) were applied between the electrodes to generate dielectric barrier discharges for 4 min. During the experiment, the Ar gas, heated to a certain temperature in the needle, was blown onto the alcohol sample and transported the volatilized alcohol to the upper plasma region. Under these conditions, the discharge power averaged approximately 20 W, which was almost the same as what had been noted for the solution plasma; the 4 min treatment time was sufficient to complete the alcohol volatilization and plasma treatment. The product gas was collected in a 10-L gas bag with the carrier gas.

2.4. Analytical Methods

The voltage and current waveforms between the electrodes were measured with a high-voltage probe (SS-0170R, Iwatsu Electric Co., Palo Alto, CA, USA) and a current monitor (Model 110, Pearson Electronics, Inc., Palo Alto, CA, USA), respectively. A high-voltage probe (P6015A, Tektronix, Inc., Tokyo, Japan) was used for the atmospheric pressure plasma treatment. The waveforms were displayed on an oscilloscope (GDS-2202A, Good Will Instrument Co., Ltd., New Taipei, Taiwan). The average of the products of the instantaneous values of current and voltage per cycle was calculated, and the result was recorded once per second as the discharge power. The solution temperature measured with the thermocouple

was recorded with a digital multimeter (GDM-8342, Good Will Instrument Co., Ltd.) When the distance between the electrodes was 1.0 mm, the discharge power was approximately 20 W regardless of the type and concentration of alcohol. The temperature of the aqueous solution increased from room temperature to >40 °C after 10 min of discharge. Appendix A shows the typical changes in discharge power and solution temperature.

The product gas in the gas bag was analyzed by using micro-gas chromatography (micro-GC, Agilent 990, Agilent Technologies Inc., Santa Clara, CA, USA) under the following conditions after adding 10 mL of Ne gas (>99.999%, Imamura Sanso Corp.) as an internal standard. Channel 1: column—MS5 A 10 m; column temperature—100 °C; inlet pressure—170 kPa. Channel 2: column—PoraPLOT Q 10 m; column temperature—80 °C; inlet pressure—190 kPa. Channel 3: column—PoraPLOT U 10 m; column temperature—80 °C; inlet pressure—190 kPa. Channel 4: column—CP-WAX 52CB 4 m; column temperature—40 °C; inlet pressure—130 kPa. In all channels, Ar was used as the carrier gas and thermal conductivity detectors were used as the detectors. When 100 mL of aqueous alcohol was placed in the solution plasma reactor, there was a total of 44 mL of empty space (filled with Ar) in the reactor and a connecting tube to the gas bag. Since this space also contained the product gas, the results reported here were corrected for the gas yield in accordance with the present authors' previous study [27]. In addition, because there was air contamination in this micro-GC system, CO_2 was slightly overestimated. Therefore, the CO_2 in the contaminated air (approximately 400 ppm) was subtracted from the CO_2 quantification results and reported. However, the effect of these corrections was small in all cases in this study.

For the spectroscopic analysis of the luminescence of the solution plasma, a simple reactor consisting of a quartz tube (inner diameter—0.9 cm; length—5.0 cm) and tungsten-rod electrodes (Figure 1c) was used. Each alcohol solution, prepared as described in Section 2.1, was placed in this reactor, and high-voltage pulses were applied as described in Section 2.2 to generate solution plasma. The plasma luminescence was received with an optical fiber and analyzed with a spectrometer (C10082CAH, Hamamatsu Photonics K.K., Hamamatsu, Japan). Since the Na concentration of each alcohol solution was known, the intensity of the obtained spectrum was adjusted based on the Na luminescence intensity and reported.

3. Results and Discussion

3.1. Decomposition of Alcohols in Solution Plasma

Figure 2 shows the micro-GC chromatograms of channels 1–3 for the product gases after the solution plasma treatment (approximately 20 W for 10 min) of each alcohol solution, with the cases of 20 wt% alcohol concentration being used as examples. Channel 1 could separate mainly inorganic gases; H_2, O_2, N_2, CH_4, and CO were detected from all the alcohol solutions along with standard Ne gas. Due to the structure of the micro-GC system, the air was always contaminated during the analysis; thus, the N_2 and O_2 were present due to air contamination. Since the ratio of N_2 to O_2 detected was always consistent with the air composition, no or negligible quantities of O_2 were generated from any of the aqueous alcohols in this study.

Channels 2 and 3 could separate mainly low-molecular-weight hydrocarbon gases (C_1–C_3). CH_4, CO_2, C_2H_2, C_2H_4, C_2H_6, H_2O, C_3H_6, and C_3H_8 were found in channel 2, and CH_4, C_2H_4, C_2H_6, C_2H_2, C_3H_6, and C_3H_8 were found in channel 3, from all the alcohol solutions. Because C_2H_2 and C_2H_4 overlapped in channel 2, and C_3H_6 and C_3H_8 overlapped in channel 3, these channels were used complementarily to quantify these hydrocarbon gases. Although H_2 was produced during solution plasma treatment even in the absence of alcohols, its quantity was small [27] and almost negligible in this study.

Figure 3 shows the micro-GC chromatograms obtained in channel 4, which could separate relatively large molecules. Acetaldehyde and some MeOH were detected from EtOH; acetaldehyde, propionaldehyde, and EtOH were detected from 1-PrOH, and as acetaldehyde and acetone were detected from 2-PrOH. An unidentified peak was also observed in EtOH, 1-PrOH, and 2-PrOH at 47 s. These detected compounds were considered

to be intermediates to gases. They are almost liquid at room temperature and tended to condense at the inlet of the micro-GC. The slightly higher intensity of acetaldehyde was probably because of its comparatively lower boiling point (20.2 °C). Therefore, the results of channel 4 indicated the presence of products, but rendered quantification difficult. These compounds remained, to some extent, at the inlet of the micro-GC and contaminated the next analysis. Therefore, the data in Figure 3 were obtained after 1 day of blank analyses to ensure that nothing was detected.
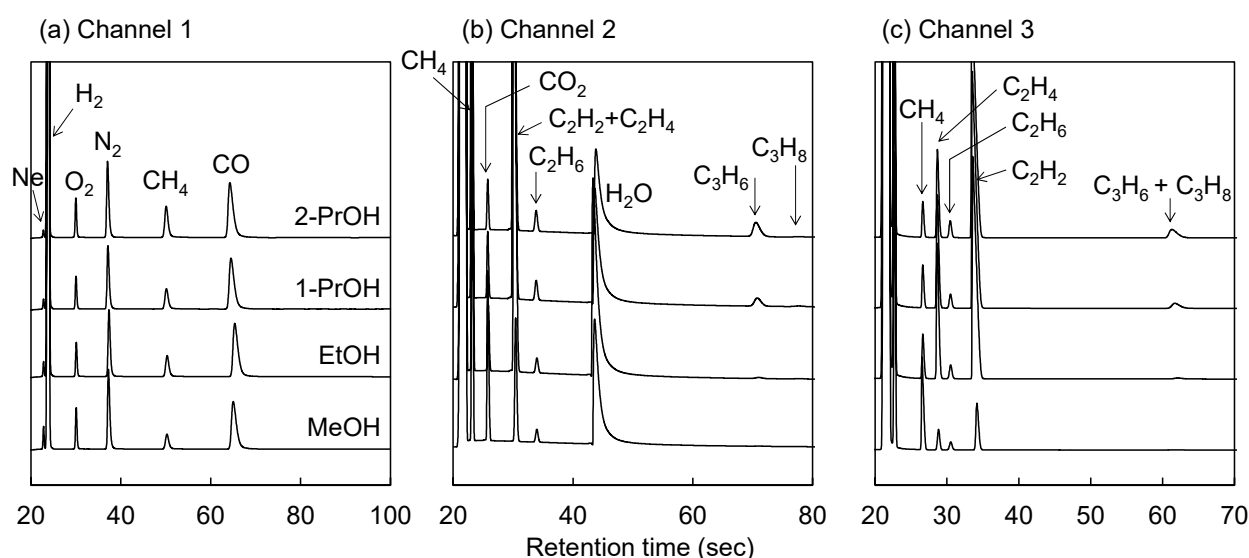
Figure 2. Micro-GC chromatograms (channels 1–3) (**a**–**c**) of the product gas from solution plasma treatment (20 W for 10 min) of aqueous alcohols (20 wt% alcohol concentration).
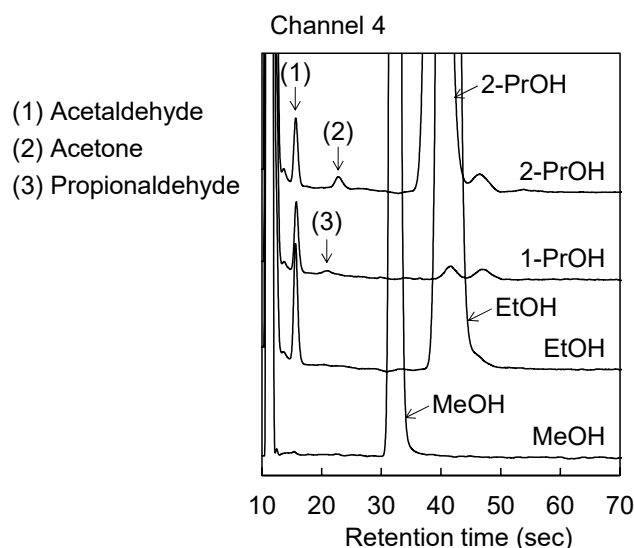

Figure 3. Micro-GC chromatograms (channel 4) of the product gas from solution plasma treatment (20 W for 10 min) of aqueous alcohols (20 wt% alcohol concentration).

The average discharge power during solution plasma treatment was ca. 20 W under the conditions of this study, but there was some variation for each experiment. In addition, as explained in Appendix A, when the alcohol concentration was >50 wt%, the solution plasma treatment time was <10 min because the start of the discharge was delayed. The present authors' previous study indicates that a higher discharge power and a longer discharge time correspond to a higher gas yield [27]. For comparison under the same

conditions, the total quantity of gas produced per level of discharge power and discharge time was evaluated [Equation (1)] and defined as the gasification rate κ_{gas}.

$$\kappa_{gas}(mol/MJ) = \frac{H_2 + CO + CO_2 + CH_4 + C_{2-3}\,hydrocarbons(mol)}{Discharge\ power(W) \times Discharge\ time(s)} \times 10^6 \quad (1)$$

Figure 4 shows the relationship between the gasification rate and alcohol concentration in the solution plasma treatment of each alcohol solution. For all alcohols, the gasification rate increased with increasing alcohol concentration, reached a maximum value at a certain concentration, and then decreased. As the alcohol concentration was further increased, the gasification rate tended to either remain constant or increase again. The experiment could not be performed at alcohol concentrations greater than those indicated in Figure 4 (>70 wt%) because there was no discharge. The alcohol concentration at which the gasification rate reached a maximum depended on the type of alcohol: for MeOH it was at 57 wt%, for EtOH at 32 wt%, and for both 1-PrOH as well as 2-PrOH, at 21 wt%.
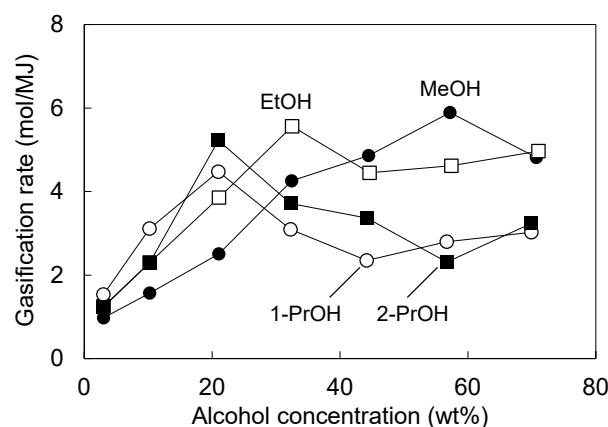

Figure 4. Gasification rates from solution plasma treatments (20 W for 10 min) of aqueous alcohols at various alcohol concentrations.

Such behavior with maximum gasification rates is likely indicative of a second-order reaction. In the simplest second-order reaction involving alcohol and water, the gasification rate would be proportional to the product of the mole fraction of alcohol (x) and that of water ($1 - x$) [Equation (2)], wherein the maximum rate is at $x = 0.5$.

$$\kappa_{gas} \propto x(1 - x) \quad (2)$$

The fact that the gasification rate had a maximum value suggests that both alcohol and water are involved in the gasification of alcohol. Because OH radicals form in the solution plasma of water [21], it is likely that in the presently reported experiments, water-derived OH radicals, not water itself, caused the gasification of the alcohols. In accordance with Equation (2), as the alcohol concentration approaches 100%, the water concentration approaches 0%; thus, in this study, the gasification rate would also have approached zero.

However, the gasification rate tended to increase again at higher alcohol concentrations. This fact suggests that a first-order reaction was also involved in the gasification pathways of the alcohols with the second-order reaction. In other words, there is likely a pathway in which only an alcohol molecule is degraded, without the influence of water. In the simplest case, the gasification rate would be proportional to the alcohol concentration (x), as below:

$$\kappa_{gas} \propto x \quad (3)$$

Consequently, the change in gasification rate with alcohol concentration in Figure 4 was considered to be attributable to a combination of first- and second-order reactions.

Figure 5 shows the composition of the gases produced from each alcohol solution. H_2 and CO were the major gases produced from all the aqueous alcohols, with small percentages of other gases. The H_2/CO ratio in the product gas was in the range of 1.4–2 for all alcohols and varied slightly with alcohol concentration, but there was no clear trend in the changes (Table 1). The H_2/CO ratios for MeOH, EtOH, and 1-PrOH tended to be close to 2, whereas that for 2-PrOH was ca. 1.5—slightly lower than that of the other alcohols.
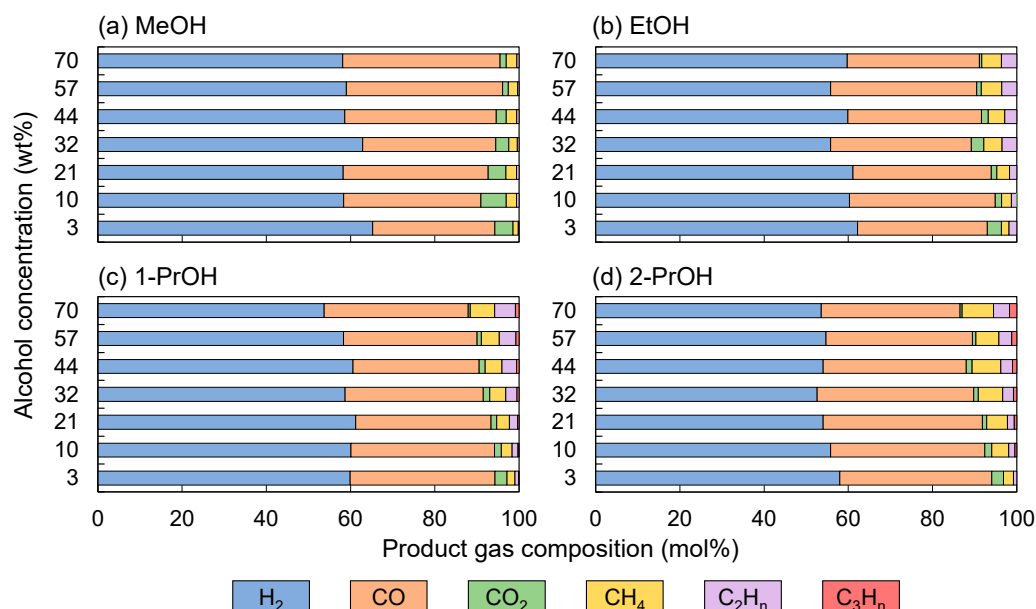
Figure 5. Product gas composition from solution plasma treatment (20 W for 10 min) of aqueous alcohols at various alcohol concentrations.

Table 1. H_2/CO ratio in the product gas from solution plasma treatment (20 W for 10 min) of aqueous alcohols.

Alcohol Concentration (wt%)	H_2/CO Ratio (mol/mol)			
	MeOH	**EtOH**	**1-PrOH**	**2-PrOH**
3	2.24	2.02	1.74	1.60
10	1.79	1.74	1.76	1.52
21	1.69	1.86	1.90	1.43
32	1.99	1.67	1.79	1.41
44	1.62	1.89	2.02	1.59
57	1.59	1.61	1.84	1.57
70	1.55	1.90	1.57	1.62

The CO_2 ratios were low for all alcohols and tended to decrease with increasing alcohol concentration, although there was some fluctuation. As discussed in a subsequent paragraph, because CO_2 was not formed during atmospheric pressure plasma treatment in the absence of water, the formation of CO_2 was attributed to the presence of water. This might have been because of the water–gas shift reaction ($CO + H_2O \rightarrow CO_2 + H_2$) [27]. The present authors assumed that a higher alcohol concentration corresponded to a lower concentration of water, thus reducing the opportunity for the water–gas shift reaction and resulting in lower CO_2 ratios. In the gasification of alcohols in supercritical water, Susanti et al. reported that the gasification of MeOH and EtOH at 740 °C/25 MPa produced H_2 and CO_2 as the main product gases, with a little CO [28]. Due to the high temperature and density of supercritical water, the water–gas shift reaction would be more pronounced. In the solution plasma process, the decomposition of alcohol was mainly in the vapor bubbles of water and alcohol, where there were gas-phase discharges [27]. Therefore, the

water–gas shift reaction would not be pronounced because of the low density of water in the reaction field.

The ratios of hydrocarbon gases such as CH_4, C_2, and C_3 were small in all of the analyzed aqueous alcohols. For MeOH (Figure 5a), the CH_4 ratio tended to increase with increasing alcohol concentration, and very small amounts of C_2 and C_3 hydrocarbons were produced. For EtOH (Figure 5b), the ratios of CH_4 and C_2 hydrocarbons tended to increase with increasing alcohol concentration, with a limited formation of C_3 hydrocarbons. For 1-PrOH and 2-PrOH (Figure 5c,d, respectively), C_3 hydrocarbons were formed to some extent in addition to CH_4 and C_2 hydrocarbons, and the ratios of these hydrocarbons increased with increasing alcohol concentration. Comparing 1-PrOH and 2-PrOH, the former produced a higher proportion of C_2 hydrocarbons, and the latter, a higher proportion of CH_4. Thus, for all alcohols, the ratios of hydrocarbon gases tended to increase with increasing alcohol concentration. This proportion to alcohol concentration is likely indicative of a first-order reaction. Combined with the discussion in Figure 4, it is clear that the C_1–C_3 hydrocarbons would have been formed solely by the decomposition of alcohol without the influence of water.

3.2. Decomposition of Alcohols in Atmospheric Pressure Plasma

Figure 6 shows the composition of the gases produced from the selected alcohols treated in atmospheric pressure plasma (approximately 20 W for 4 min) without water. The solution plasma used in this study is a gas-phase discharge that occurs in vapor bubbles generated by the volatilization of water and alcohol by Joule heating [27]. Both the atmospheric pressure plasma and the solution plasma in this study were gas-phase discharges, with the main difference between them being the presence/absence of water.
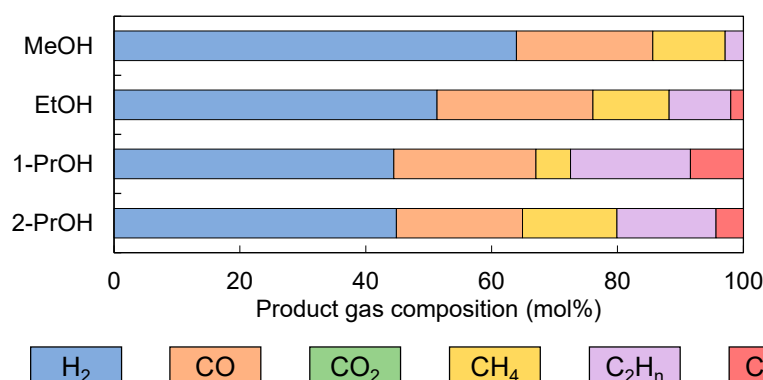

Figure 6. Product gas composition from atmospheric pressure plasma treatment (20 W for 4 min) of neat alcohols.

Similar to what had occurred in the solution plasma treatment, H_2 and CO were the first and second major gases produced, respectively, but the ratios of C_1–C_3 hydrocarbon gases were substantially larger than what had been noted in the case of the solution plasma. The percentages of hydrocarbon gases were even larger for alcohols with higher numbers of carbon atoms. Comparing 1-PrOH and 2-PrOH, the former produced C_2 hydrocarbons in higher ratios, whereas the latter produced more CH_4; this tendency was similar to what had been noted in the case of the solution plasma. Thus, the ratios of hydrocarbon gases in the product gas were large under the atmospheric pressure plasma treatment in the absence of water. Therefore, the increase in hydrocarbon gases with alcohol concentration in solution plasma (Figure 5) can be attributed to an increase in decomposition reactions in which water is not involved. As suggested in a subsequent paragraph, this is probably because of gasification pathways in which solely the alcohol decomposes. In the case of the atmospheric plasma treatment, no CO_2 was produced; as discussed in Section 3.1, the production of CO in solution plasma would have certainly occurred because of the water–gas shift reaction.

3.3. Plasma Emission Spectroscopy

Using the reactor shown in Figure 1c, the emission from solution plasma was analyzed spectroscopically. Since there were no substantial differences between the alcohols, only the spectra of aqueous 2-PrOH are shown in Figure 7. The spectra for other alcohols are shown in Appendix B (Figure A2). Each peak was assigned according to the literature [29]. Emissions from chemical species such as OH, C-C, H, O, and Na were observed in the spectra. The intensities of the emission from OH radicals at 260.9, 281.1, 287.1, 306.4, and 342.8 nm weakened as the alcohol concentration increased (i.e., as the water concentration decreased), and became almost nondetectable at an alcohol concentration of 70 wt%. This indicates that most of the OH radicals in the plasma had originated from water and none from the alcohols. The H and O peaks were similar to OH, and most of these would have also come from water. The contribution of OH radicals to the decomposition of EtOH in solution plasma was also mentioned by Zhao et al. [21].
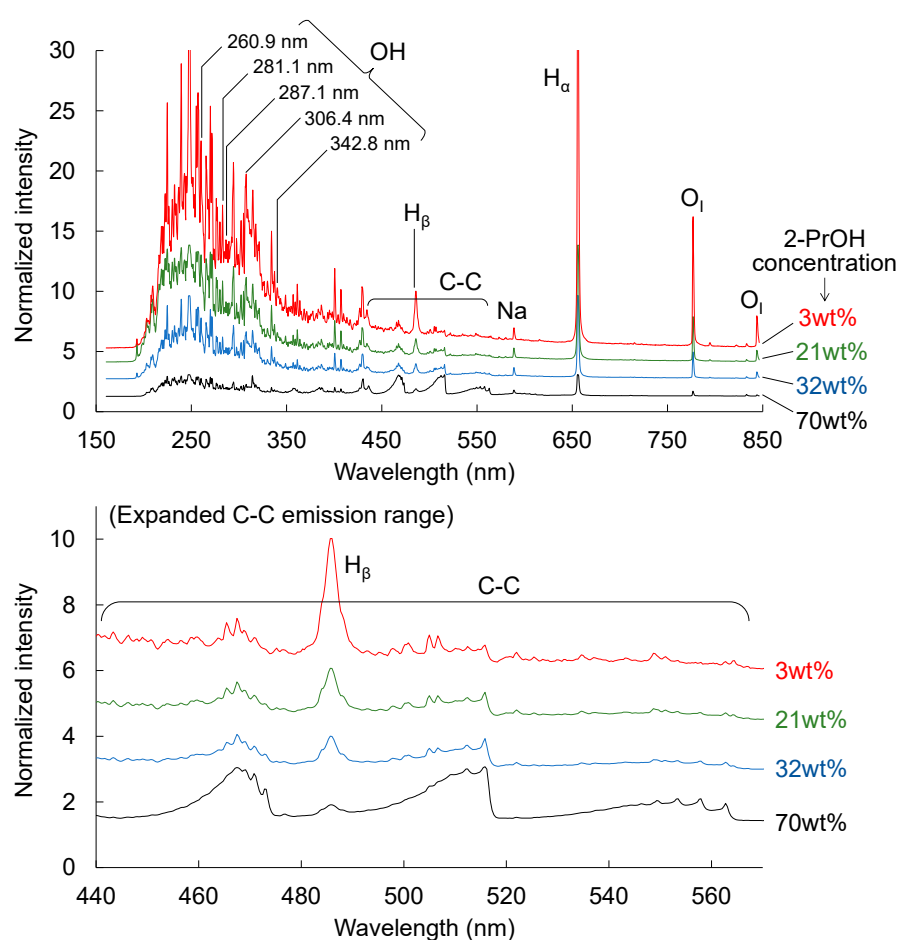
Figure 7. Emission spectrum from solution plasma of aqueous 2-PrOH. (The emission intensity was normalized to the Na intensity at 0 wt% alcohol concentration.).

In Section 3.1, the second-order reaction was discussed as a reason for the gasification rate having a maximum value. Figure 7 indicates that OH radicals were generated almost proportionally to the water concentration, indicating that the gasification of alcohols with OH radicals might have led to the behavior reminiscent of a second-order reaction.

To further discuss the reaction between alcohols and OH radicals, it must be noted that the O/C ratio of the product gas was calculated from the gas composition in Figure 5 (Table 2). The O/C ratio of the product gas from MeOH was ca. 1 at any MeOH concentration. Since the O/C ratio of the MeOH molecule (CH_3OH) was also 1, this result was reasonable regardless of the decomposition path.

Table 2. O/C ratio of product gas from solution plasma treatment (20 W for 10 min) of aqueous alcohols. The O/C ratio of each alcohol molecule is shown in parentheses.

Alcohol Concentration (wt%)	O/C Ratio (mol/mol) of the Product Gas			
	MeOH (O/C = 1.00)	EtOH (O/C = 0.50)	1-PrOH (O/C = 0.33)	2-PrOH (O/C = 0.33)
3	1.09	0.95	0.87	0.99
10	1.07	0.93	0.90	0.86
21	1.02	0.88	0.85	0.82
32	1.01	0.83	0.81	0.77
44	0.96	0.82	0.75	0.73
57	0.97	0.78	0.74	0.73
70	0.96	0.74	0.67	0.65

The O/C ratios of EtOH (C_2H_5OH), 1-PrOH, and 2-PrOH (C_3H_7OH) molecules were 0.5, 0.33, and 0.33, respectively, but the O/C ratios of the product gas were all close to 1. The excess O atoms in the product gas, as compared with the number of O atoms in the feedstock, should have originated from the O atoms of water molecules. The O/C ratio of the product gas being close to 1 indicates that most of the C atoms of the alcohols were combined with O atoms, suggesting a strong influence of OH radicals from water. In addition, for EtOH, 1-PrOH, and 2-PrOH, the O/C ratio decreased monotonically from 1 with increasing alcohol concentration. This decrease might have been because of the decrease in OH radicals from water, and thus, the decrease in the decomposition path with OH radicals. As shown in Figure 7, the intensities of C–C emissions increased with increasing alcohol concentration, corresponding to the increase in hydrocarbon gases in Figure 5; this might have been because of the increase in the frequency of the sole decomposition of alcohol.

Instead of the O/C ratio of alcohol molecules, the O/C ratio of aqueous alcohol can be discussed. The O/C ratio of aqueous alcohol is large, especially in dilute solutions. For example, the O/C ratio is 58.5 (mol/mol) in a 3 wt% methanol solution and 2.8 in a 50 wt% methanol solution; these values are very different from the ratio of the product gas. Therefore, gas production is not related to the O/C ratio of an aqueous alcohol solution.

3.4. Proposed Decomposition Pathway of Alcohols in Solution Plasma

Considering these lines of evidence and discussion, the solution plasma treatment of alcohols might have involved two degradation pathways: (a) the oxidative decomposition with OH radicals from water and (b) the decomposition of solely the alcohol molecule. The former is a second-order reaction and the latter is a first-order reaction, and their combination can explain the changes in gasification rate shown in Figure 4. For example, Figure 8 suggests possible decomposition pathways for 1-PrOH. In pathway (a), 1-PrOH undergoes the abstraction of an H atom by an OH radical and decomposes in a manner that forms propionaldehyde (which was found in the micro-GC analysis (Figure 3)), followed by decarbonylation in a manner that forms an ethyl radical. If the OH radicals are abundant in the reaction system, the ethyl radical can couple with an OH radical in a manner that forms EtOH. This pathway produces two H_2 molecules and one CO molecule, whereas the alcohol reduces one carbon chain as follows.

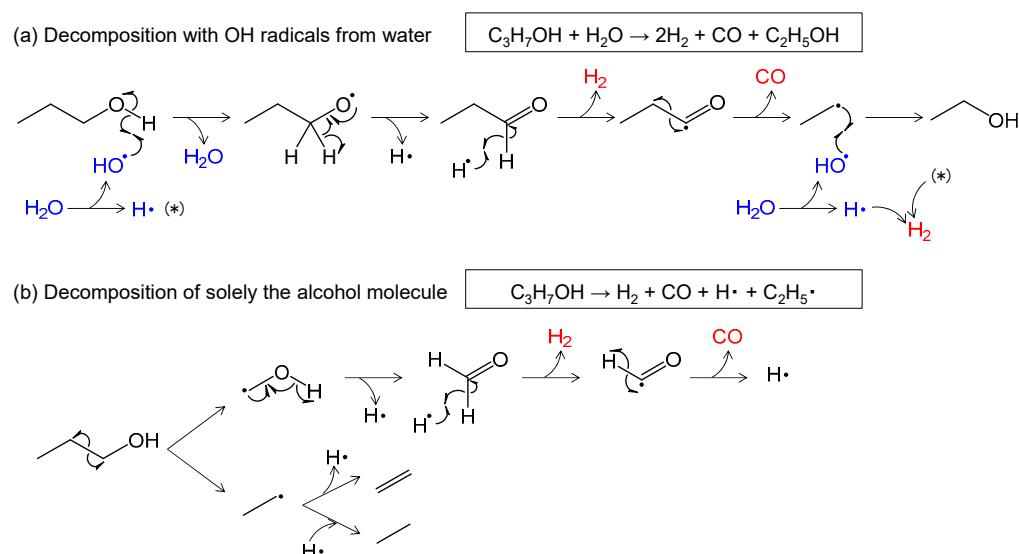$$C_3H_7OH + H_2O \rightarrow 2H_2 + CO + C_2H_5OH \tag{4}$$
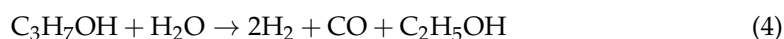
Figure 8. Possible decomposition pathways of 1-PrOH in solution plasma.

A similar pathway can be provided for EtOH and MeOH (Appendix C, Figures A3a and A4a), respectively. Thus, with a strong contribution of OH radicals from water, 1-PrOH can be completely gasified stepwise via EtOH and MeOH, eventually producing H_2 and CO in a 2:1 ratio. The net reaction for the complete gasification of 1-PrOH by this pathway (a) is as follows.

$$C_3H_7OH + 2H_2O \rightarrow 6H_2 + 3CO \tag{5}$$

Table 1 indicates that the H_2/CO ratios of the product gases from MeOH, EtOH, and 1-PrOH were ca. 2. Although there is currently no direct evidence to support this pathway, it can explain the composition of the product gas and the intermediates. However, for the ethyl radical to couple with the OH radical in this pathway, the OH radicals would have to be abundant relative to the water. More research and direct evidence are needed to clarify this point.

In pathway (b), a homolytic C–C bond cleavage, probably caused by collision with a high-energy electron, decomposes 1-PrOH into a hydroxymethyl radical and an ethyl radical. The former gasifies via formaldehyde in a manner that forms H_2 and CO, whereas the latter produces either ethylene or ethane. The reaction equation for this pathway (b) is as follows.

$$C_3H_7OH \rightarrow H_2 + CO + H\cdot + C_2H_5 \tag{6}$$
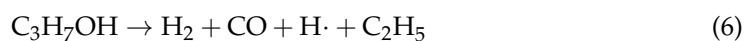
CH_4 and C_3 hydrocarbons were also produced in Figure 5c, and they could have been formed if either the terminal C–C bond or the C–O bond were cleaved first. A similar pathway can be given for EtOH (Figure A3b). Thus, pathway (b) for 1-PrOH and EtOH (Figures 8b and A3b, respectively) eventually produces H_2 and CO in a 1:1 ratio with some hydrocarbon gases. Since MeOH produces two H_2 molecules and one CO molecule in pathway (b) (Figure A4b), the result is the same as in pathway (a) (Figure A4a). These pathways, in which solely alcohol decomposes without OH radicals, can explain the fact that the concentration of hydrocarbon gases increased when the alcohol concentration was high.

The degradation pathway for 2-PrOH is likely slightly different (Figure 9). In pathway (a), an OH radical abstracts an H atom from 2-PrOH in a manner that forms acetone, which is further gasified by decarbonylation via an acetaldehyde radical. This pathway yields H_2 and CO in a 2:1 ratio with two methyl radicals. If all two methyl radicals couple with OH radicals in a manner that forms two MeOH molecules, the net reaction is represented by the equation below.
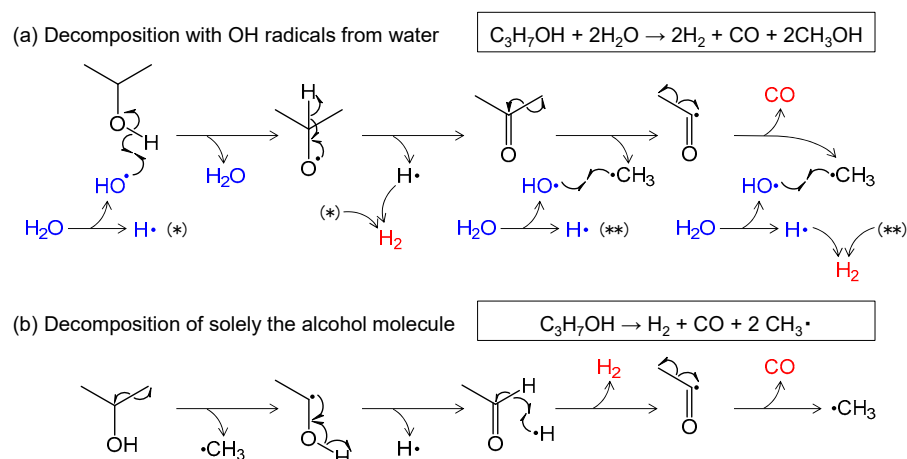
$$C_3H_7OH + 2H_2O \rightarrow 2H_2 + CO + 2CH_3OH \tag{7}$$
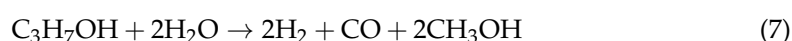
Figure 9. Possible decomposition pathways of 2-PrOH in solution plasma.

The produced MeOH will also further decompose into H_2 and CO in a 2:1 ratio (Figure A4), but many OH radicals are required in this pathway (Figure 9a) compared with the case of 1-PrOH (Figure 8a). Therefore, the frequency of methyl radicals coupling with other radicals such as H could increase, leading to an increase in CH_4 (Figure 5d) and a decrease in H_2 (Table 1). In pathway (b), however, 2-PrOH produces H_2 and CO in a 1:1 ratio via an acetaldehyde radical, and two methyl radicals are also produced as follows.

$$C_3H_7OH \rightarrow H_2 + CO + 2CH_3 \qquad (8)$$
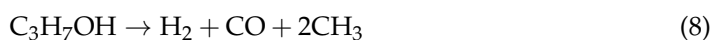
In this pathway, where no OH radicals are involved, these methyl radicals are converted into hydrocarbons. Thus, pathways (a) and (b) in Figure 9 can explain the composition of the product gas and intermediates (acetone and acetaldehyde) from 2-PrOH.

Again, the pathways proposed in Figures 8 and 9 are examples that can explain the products and intermediates without contradiction, although there has not yet been any direct evidence for them. In any case, H_2 and CO are the main product gases, and a strong contribution of OH radicals would lead the H_2/CO ratio to approach 2 and the O/C ratio to approach 1 in the product gas from any of the alcohols studied.

4. Conclusions

This study found that solution plasma treatment with water can produce gases that are rich in H_2 and CO (from methanol, ethanol, and 1-propanol, in a ratio of ca. 2:1, and from 2-propanol in a ratio of 1.5:1). Since H_2 and CO were the major product gases in the conducted experiments, the O/C ratio was close to 1 for each alcohol, indicating that most of the carbon atoms in the alcohol carbon chain were bonded to O atoms. This excess of O atoms could only have been derived from water, suggesting a strong contribution of OH radicals from water to alcohol gasification.

The gasification rate, defined as the quantity of gas produced per unit of electricity (moles per megajoule), had a maximum value at a certain alcohol concentration: methanol at 57 wt%, ethanol at 32 wt%, and both 1- as well as 2-propanol at 21 wt%. The reason for this maximum could be explained by a second-order reaction with alcohol and OH radicals from water. The ratios of C_1–C_3 hydrocarbons in the product gas was small for each alcohol, but exhibited a tendency to increase with alcohol concentration. This increase could be explained by a first-order reaction because of the decomposition of solely alcohol.

Possible decomposition pathways have been proposed for second-order reactions with OH radicals and first-order reactions solely with alcohols. The former pathway assumes the presence of abundant OH radicals (at a higher concentration than that of the water) in the reaction system. A remaining issue is to obtain direct evidence of this interpretation, but these proposed pathways provide an explanation that is consistent with the experimental

facts such as the product gas composition, changes in gasification rate, and intermediates detected. To obtain direct evidence of the reaction pathway, solution plasma treatment with a water isotope such as water-^{17}O would be helpful.

From an economic point of view, the cost of hydrogen is related to the production volume per unit time, and the gasification rate defined in this study is an indicator that can be used to evaluate it. This study showed that there is an optimum alcohol concentration at which the gasification rate is maximized. The results of this study will be useful in establishing more economical hydrogen production in solution plasma.

Appendix A

Figure A1 shows two typical examples of changes in discharge power and solution temperature during solution plasma treatment. The discharge power is the average of 10 one-cycle power values recorded once per second, and the upper and lower error bars indicate the sample standard deviation. When the alcohol concentration was not high (Figure A1a, 10 wt% EtOH), the discharge started immediately after the high-voltage pulses were applied, and the power was almost constant from 0–10 min; in this case, it amounted to slightly >20 W. However, when the alcohol concentration was >50 wt% (Figure A1b, 57 wt% EtOH), there was no discharge in the early stage of the treatment, and there was only Joule heating, resulting in low power. After the solution temperature increased to some extent, the discharge started, and the power increased to nearly 20 W. Thus, when the alcohol concentration was high, the start of the discharge was delayed because the conductivity of the solution (i.e., from the low NaCl concentration) was low, which weakened the Joule heating between the electrodes. In such cases, the solution plasma treatment was <10 min, but the gasification rate was evaluated in this study by omitting this Joule heating period.
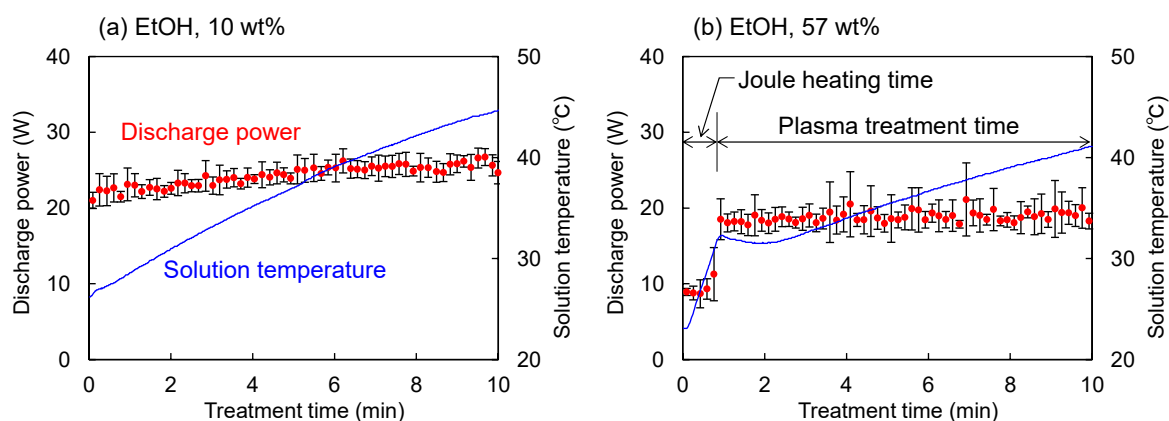

Figure A1. Changes in discharge power and solution temperature during solution plasma treatment of (**a**) 10 wt% and (**b**) 57 wt% aqueous EtOH.
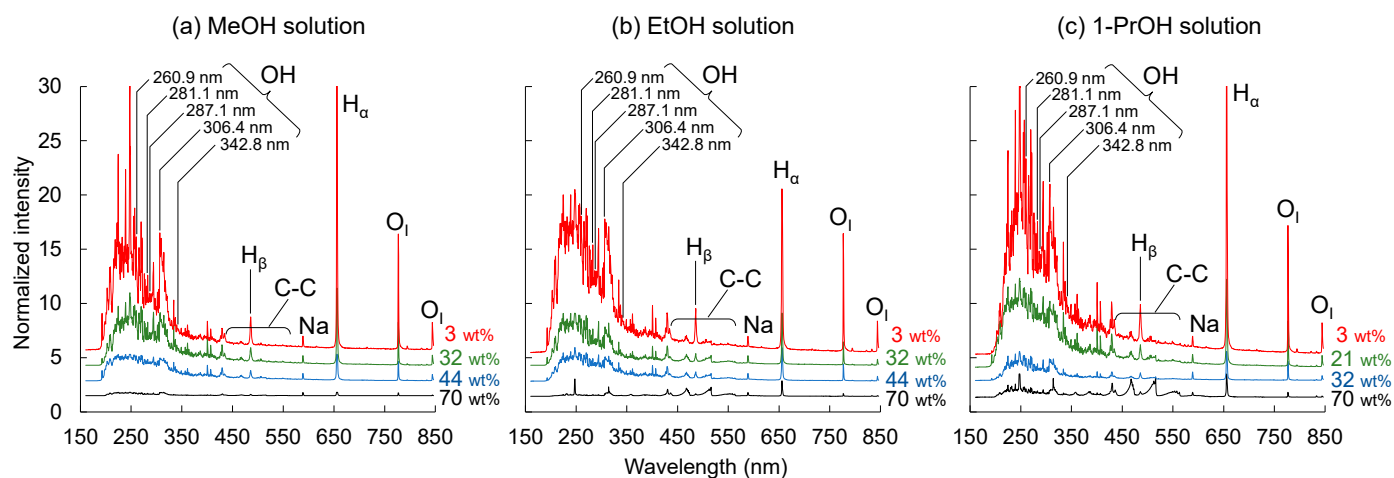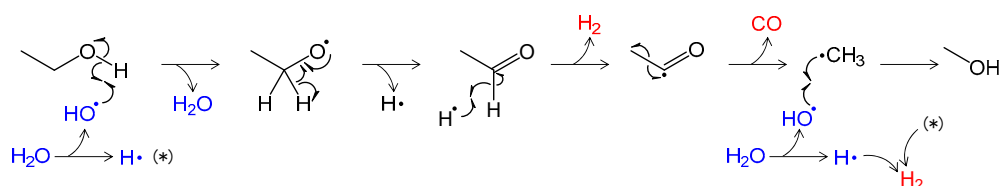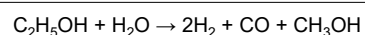
Appendix B

Figure A2. Emission spectra from solution plasma of aqueous (**a**) MeOH, (**b**) EtOH, and (**c**) 1-PrOH. (The emission intensity was normalized to the Na intensity at 0 wt% alcohol concentration.).

Appendix C

(a) Decomposition with OH radicals from water $C_2H_5OH + H_2O \rightarrow 2H_2 + CO + CH_3OH$

(b) Decomposition of solely the alcohol molecule $C_2H_5OH \rightarrow H_2 + CO + H\cdot + CH_3\cdot$
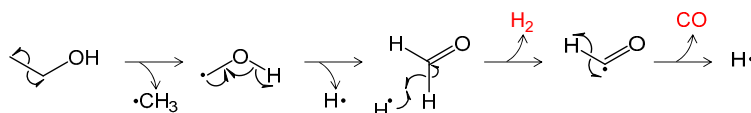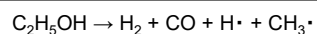
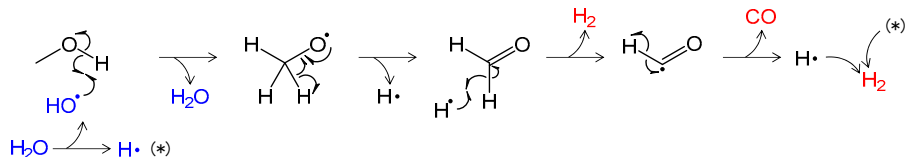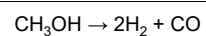**Figure A3.** Possible decomposition pathways of EtOH in solution plasma.

(a) Decomposition with OH radicals from water $CH_3OH \rightarrow 2H_2 + CO$

(b) Decomposition of solely the alcohol molecule $CH_3OH \rightarrow 2H_2 + CO$
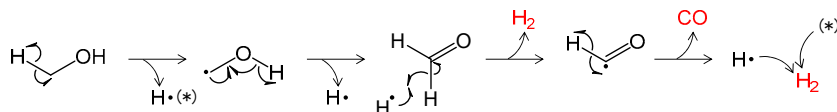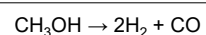

Figure A4. Possible decomposition pathways of MeOH in solution plasma.

References

1. Palanisamy, A.; Soundarrajan, N.; Ramasamy, G. Analysis on production of bioethanol for hydrogen generation. *Environ. Sci. Pollut. Res.* **2021**, *28*, 63690–63705. [CrossRef] [PubMed]
2. Kumar, S.S.; Lim, H. An overview of water electrolysis technologies for green hydrogen production. *Energy Rep.* **2022**, *8*, 13793–13813. [CrossRef]
3. Vuppaladadiyam, A.K.; Vuppaladadiyam, S.S.V.; Awasthi, A.; Sahoo, A.; Rehman, S.; Pant, K.K.; Murugavelh, S.; Huang, Q.; Anthony, E.; Fennel, P.; et al. Biomass pyrolysis: A review on recent advancements and green hydrogen production. *Bioresour. Technol.* **2022**, *364*, 128087. [CrossRef] [PubMed]
4. Inayat, A.; Tariq, R.; Khan, Z.; Ghenai, C.; Kamil, M.; Jamil, F.; Shanableh, A. A comprehensive review on advanced thermo-chemical processes for bio-hydrogen production via microwave and plasma technologies. *Biomass Convers. Biorefinery* **2020**, 1–10. [CrossRef]
5. Arpia, A.A.; Nguyen, T.B.; Chen, W.H.; Dong, C.D.; Ok, Y.S. Microwave-assisted gasification of biomass for sustainable and energy-efficient biohydrogen and biosyngas production: A state-of-the-art review. *Chemosphere* **2022**, *287*, 132014. [CrossRef]
6. Ulejczyk, B.; Nogal, L.; Mlotek, M.; Krawczyk, K. Efficient Plasma Technology for the Production of Green Hydrogen from Ethanol and Water. *Energies* **2022**, *15*, 2777. [CrossRef]
7. Ni, M.; Leung, D.Y.C.; Leung, M.K.H. A review on reforming bio-ethanol for hydrogen production. *Int. J. Hydrogen Energy* **2007**, *32*, 3238–3247. [CrossRef]
8. Zike, Q.; Xiange, W.; JianMin, M.; JiaMin, D.; ChangMing, D. Green hydrogen from bio-ethanol reforming using micro plasma. *Waste Dispos. Sustain. Energy* **2020**, *2*, 15.
9. Du, C.M.; Li, H.X.; Zhang, L.; Wang, J.; Huang, D.W.; Xiao, M.D.; Cai, J.W.; Chen, Y.B.; Yan, H.L.; Xiong, Y. Hydrogen production by steam-oxidative reforming of bio-ethanol assisted by Laval nozzle arc discharge. *Int. J. Hydrogen Energy* **2012**, *37*, 8318–8329. [CrossRef]
10. Du, C.M.; Mo, J.M.; Li, H.X. Renewable Hydrogen Production by Alcohols Reforming Using Plasma and Plasma-Catalytic Technologies: Challenges and Opportunities. *Chem. Rev.* **2015**, *115*, 1503–1542. [CrossRef]
11. Takai, O. Solution plasma processing (SPP). *Pure Appl. Chem.* **2008**, *80*, 2003–2011. [CrossRef]
12. Akyuz, A.; Ozkan, M. Degradation of Polyvinylpyrrolidone by Solution Plasma Process. *Acta Phys. Pol. A* **2017**, *131*, 343–345. [CrossRef]
13. Mun, M.K.; Lee, W.O.; Park, J.W.; Kim, D.S.; Yeom, G.Y.; Kim, D.W. Nanoparticles Synthesis and Modification using Solution Plasma Process. *Appl. Sci. Converg. Technol.* **2017**, *26*, 164–173. [CrossRef]
14. Hieda, J.; Shirafuji, T.; Noguchi, Y.; Saito, N.; Takai, O. Solution Plasma Surface Modification for Nanocarbon-Composite Materials. *J. Jpn. Inst. Met.* **2009**, *73*, 938–942. [CrossRef]
15. Sun, B.; Sato, M.; Clements, J.S. Optical study of active species produced by a pulsed streamer corona discharge in water. *J. Electrost.* **1997**, *39*, 189–202. [CrossRef]
16. Xin, Y.B.; Sun, B.; Zhu, X.M.; Yan, Z.Y.; Liu, Y.J.; Liu, H. Characteristics of hydrogen produced by pulsed discharge in ethanol solution. *Appl. Energy* **2016**, *168*, 122–129. [CrossRef]
17. Sun, B.; Zhao, X.T.; Xin, Y.B.; Zhu, X.M. Large capacity hydrogen production by microwave discharge plasma in liquid fuels ethanol. *Int. J. Hydrogen Energy* **2017**, *42*, 24047–24054. [CrossRef]
18. Zhu, T.H.; Sun, B.; Zhu, X.M.; Wang, L.R.; Xin, Y.B.; Liu, J.L. Mechanism analysis of hydrogen production by microwave discharge in ethanol liquid. *J. Anal. Appl. Pyrolysis* **2021**, *156*, 105111. [CrossRef]
19. Wang, B.; Sun, B.; Zhu, X.M.; Yan, Z.Y.; Liu, Y.J.; Liu, H.; Liu, Q. Hydrogen production from alcohol solution by microwave discharge in liquid. *Int. J. Hydrogen Energy* **2016**, *41*, 7280–7291. [CrossRef]
20. Xin, Y.B.; Sun, B.; Zhu, X.M.; Yan, Z.Y.; Zhao, X.T.; Sun, X.H. Hydrogen production from ethanol decomposition by pulsed discharge with needle-net configurations. *Appl. Energy* **2017**, *206*, 126–133. [CrossRef]
21. Zhao, X.T.; Sun, B.; Zhu, T.H.; Zhu, X.M.; Yan, Z.Y.; Xin, Y.B.; Sun, X.H. Pathways of hydrogen-rich gas produced by microwave discharge in ethanol-water mixtures. *Renew. Energy* **2020**, *156*, 768–776. [CrossRef]
22. Li, Y.Y.; Zhou, R.S.; Qi, F.; Zhou, D.J.; Zhou, R.W.; Wan, J.J.; Xian, Y.B.; Cullen, P.J.; Lu, X.P.; Ostrikov, K. Plasma-enabled liquid ethanol conversion for hydrogen production: Discharge characteristics and process control. *J. Phys. D-Appl. Phys.* **2020**, *53*, 174001. [CrossRef]
23. Franclemont, J.T.; Fan, X.R.; Li, R.; Singh, R.K.; Holsen, T.M.; Thagard, S.M. Chemical reaction mechanisms accompanying pulsed electrical discharges in liquid methanol. *Plasma Process. Polym.* **2018**, *15*, 1800019. [CrossRef]
24. Shiraishi, R.; Nomura, S.; Mukasa, S.; Nakano, R.; Kamatoko, R. Effect of catalytic electrode and plate for methanol decomposition by in-liquid plasma. *Int. J. Hydrogen Energy* **2018**, *43*, 4305–4310. [CrossRef]
25. Xin, Y.B.; Sun, B.; Zhu, X.M.; Yan, Z.Y.; Liu, H.; Liu, Y.J. Effects of plate electrode materials on hydrogen production by pulsed discharge in ethanol solution. *Appl. Energy* **2016**, *181*, 75–82. [CrossRef]
26. Xin, Y.B.; Wang, Q.L.; Sun, J.B.; Sun, B. Plasma in aqueous methanol: Influence of plasma initiation mechanism on hydrogen production. *Appl. Energy* **2022**, *325*, 119892. [CrossRef]
27. Minami, E.; Miyamoto, T.; Kawamoto, H. Decomposition of Saccharides and Alcohols in Solution Plasma for Hydrogen Production. *Hydrogen* **2022**, *3*, 339–347. [CrossRef]

28. Susanti, R.F.; Dianningrum, L.W.; Yum, T.; Kim, Y.; Lee, Y.W.; Kim, J. High-yield hydrogen production by supercritical water gasification of various feedstocks: Alcohols, glucose, glycerol and long-chain alkanes. *Chem. Eng. Res. Des.* **2014**, *92*, 1834–1844. [CrossRef]

29. Daidoji, H. Kaen wo mochiita bunkou-bunseki gijutsu (Flame Spectroscopic Analysis Technique). In *Kaen no Bunkougakuteki-Keisoku to Sono Ouyo (Spectroscopic Measurement of Flames and Its Applications)*, 1st ed.; Koda, S., Takubo, Y., Eds.; Japan Scientific Societies Press: Tokyo, Japan, 1990; pp. 111–159. (In Japanese)